Published in final edited form as:
Nanoscale. 2011 March ; 3(3): 963–966. doi:10.1039/c0nr00823k.

Composition Tuning the Upconversion Emission in $NaYF_4$:Yb/Tm Hexaplate Nanocrystals

Hua Zhang[a], **Yujing Li**[a], **Yungchen Lin**[a], **Yu Huang**[a,c], and **Xiangfeng Duan**[b,c]

Yu Huang: yhuang@seas.ucla.edu; Xiangfeng Duan: xduan@chem.ucla.edu

Department of Materials Science and Engineering, University of California, Los Angeles, CA 90095, U. S. A

[b]Department of Chemistry and Biochemistry, University of California, Los Angeles, CA 90095, U. S. A

[c]California Nanosystems Institute, University of California, Los Angeles, CA 90095, U. S. A

Abstract

Single crystal hexagonal $NaYF_4$:Yb/Tm nanocrytstals have been synthesized with uniform size, morphology and controlled chemical composition. Spectroscopic studies show that these nanocrystals exhibit strong energy upconversion emission when excited with a 980 nm diode laser, with two primary emission peaks centered around 452 nm and 476 nm. Importantly, the overall and relative emission intensity at these wavelengths can be readily tuned by controlling the concentration of the trivalent rare earth element dopants at the beginning of the synthesis which has been confirmed by EDX for the first time. Through systematic studies, the optimum rare earth ion doping concentration can be determined for the strongest emission intensity at the selected peak(s). Confocal microscope studies show that the upconversion emission from individual NCs can be readily visualized. These studies demonstrate a rational approach for fine tuning the upconversion properties in rare-earth doped nanostructures, and can broadly impact areas ranging from energy harvesting, energy conversion to biomedical imaging and therapeutics.

When a medium emits fluorescence as a result of being excited with incident light, the wavelength of the fluorescence is usually longer than that of the excitation light which is called down-conversion.[1] However, under some special circumstances, one can observe upconversion fluorescence, in which the wavelength of the emitted light is shorter than that of the excitation light.[2,3] This unique property makes upconversion materials attractive for a wide range of applications due to their potential for biomedical imaging and therapeutics.[4–7] In particular, the fact that they can be excited with infrared light makes them attrative candidates as biological probes for deeper imaging with lower noise, in contrast to traditional organic dyes and quantum dots.[8–11] Recently, considerable efforts have been devoted to the synthesis of energy upconversion nanoparticles.[12,13]

Trivalent rare earth element (RE^{3+}) doped materials are among the most promising materials for energy upconversion because they have multiple long-lived excited states and can exhibit highly efficient energy transfer processes that are responsible for upconversion emission under certain conditions.[2,3,14,.15,16] Here we focus our efforts on Yb-Tm doped systems that can emit violet (452 nm) or blue (476 nm) light. The ability to achieve this shorter wavelength emission is of significance for activating certain chemical or biological

Correspondence to: Yu Huang, yhuang@seas.ucla.edu; Xiangfeng Duan, xduan@chem.ucla.edu.

processes. For example, the 476 nm light can be used to excite channelrhodopsins, which are a subfamily of opsin proteins that function as light-gated ion channels in neural cells.[17] Therefore, it is important that the emission wavelength can be tuned by introducing different dopants or doping ratios. By varing the the exact doping concentration during the chemical synthesis process, we show the overall and relative emission intensity of the selected spectral peaks can be readily tuned.

$NaYF_4$ can adopt either a cubic or hexagonal structure.[12,15,18] It is well known that hexagonal structure is the more efficient matrix for upconversion phosphors.[19–21] However, most synthetic approaches result in the cubic phase $NaYF_4$/$NaYbF_4$.[22–24] Here we dicuss the synthesis of $NaYF_4$ hexplate nanocrystals (NCs) through a solution chemical approach at high temperature.

The synthesis was carried out with standard oxygen-free procedures as reported before[25,26] and all chemicals were purchased from Sigma-Aldrich and used without further purification. In a typical procedure, a certain amount of yttrium(III) oxide (Y_2O_3, 99.99%), ytterbium(III) oxide (Yb_2O_3, 99.9%) and thulium(III) oxide (Tm_2O_3, 99.9%) (1.25 mmol in all with the relative ratio depending on the exact doping concentration) were dissolved in 5 mL trifluoroacetic acid (TFA, 99%) in a 100 mL three-necked flask. The slurry was then heated to 80 °C with vigorous magnetic stirring under vacuum for 30 minutes to remove water and excessive TFA. Next, 2.5 mmol sodium trifluoroacetate ($NaCOOCF_3$, 98%) was added, along with 7.5 mL of oleic acid (OA, 90%) and 7.5 mL of 1-octadecene (ODE, 90%) at 100 °C. Afterwards, the solution was heated to 330 °C with a rate of 30 °C min^{-1} and maintained at 330 °C for 60 minutes to obtain the NCs.

The microstructures, morphologies and compositions of the $NaYF_4$:Yb/Tm NCs were characterized by a JEOL 6700 FEG scanning electron microscope (SEM) with an energy-dispersive X-ray spectroscopy (EDX). The microstructures and lattice images of $NaYF_4$:Yb/Tm NCs were observed by an FEI CM120 transmission electron microscope (TEM) and an FEI Titan high-resolution transmission electron microscope (HRTEM). Room temperature photoluminescence spectra were collected on a Spec-10® system from Princeton Instruments including a liquid nitrogen cooled CCD camera (Spectra Pro® 2300i, Model: 7509-0001). Confocal photoluminescence images were taken on a Leica TCS-SP2 AOBS inverted Confocal and Multiphoton Microscope (Mannheim, Germany) equipped with a Spectra-Physics MaiTai picosecond pulsed infrared laser (Mountain View, CA) set at 980 nm for infrared excitation.

The SEM and TEM image shows that the $NaYb_{0.99}Tm_{0.01}F_4$ NCs have a hexagonal plate structure with nearly mono-dispersed sizes (Fig. 1a,b). The diagonal length of the hexagonal plate is about 180 nm with a thickness of 50 nm. The well-defined hexagonal morphology of the NCs suggests that they are single crystals. Indeed, the HRTEM and SAED images confirmed that the as-prepared NCs are single crystals with a hexagonal phase. The lattice spacing of 5.13 Å in HRTEM image corresponds to (100) lattice planes (Fig. 1c and inset).

Although the upconversion emission peak positions usually cannot be changed for a given upconversion material, the emission efficiency at different wavelengths can be greatly affected by the exact doping concentrations. To this end, we have carried out systematic studies to control the rare earth element doping concentration in these nanocrystals. Importantly, our studies show that the doping concentration in the final NC product is directly correlated to the initial reactant ratio. For example, we have prepared a series of $NaY_{0.8-x}Yb_{0.2}Tm_xF_4$ and $NaYb_{1-x}Tm_xF_4$ NCs with variable Tm^{3+} ion concentrations. The plot of the Tm^{3+} concentration in the NCs vs. the starting reactant ratio shows a clear linear relation with a slope close to one (Fig. 2). These studies demonstrate that all the rare earth

elements can be effectively incorporated into the final NCs with our synthetic conditions. Therefore, the RE^{3+} doping concentration can be readily controlled by varying the initial reactant ratio. The size, morphology and dispersity of the NCs of variable compositions remained similar to what have been shown in Fig. 1.

In RE^{3+} doped materials, the energy transfer process between adjacent ions is the primary reason responsible for the upconversion emission. Therefore, a close match between different transition levels of the rare earth ions can critically impact the probability of energy transfer process and the efficiency of the upconversion process. In the Yb-Tm co-doped materials, the infrared radiation can be efficiently converted into blue emission by a three-photon process or violet emission by a four-photon upconversion process due to the existence of multiple energy resonances in the system (Fig. 3). One energy transfer step from Yb^{3+} ion to Tm^{3+} ion populates the $^3H_5$ level of Tm^{3+} from $^3H_6$. The $^3H_5$ decays rapidly to the $^3F_4$ level. The second energy transfer step raises the Tm^{3+} ion from $^3F_4$ to $^3F_2$ that quickly decays to $^3H_4$. Subsequently, the third transfer step raises the Tm^{3+} ion from $^3H_4$ to $^1G_4$ that can yield a blue emission upon radiative relaxation back to $^3H_6$. A fourth energy transfer step from Yb^{3+} ion to Tm^{3+} ion may also take place to populate the Tm^{3+} ion from $^1G_4$ to $^1D_2$, which is however usually less efficient due to relative large energy mismatch. An alternative way to populate $^1D_2$ is through cross relaxation between adjacent Tm^{3+} ions with three possible routes: $^3F_2 \rightarrow {}^3H_6$ and $^3H_4 \rightarrow {}^1D_2$; $^1G_4 \rightarrow {}^3F_4$ and $^3H_4 \rightarrow {}^1D_2$; and $^1G_4 \rightarrow {}^1D_2$ and $^3H_4 \rightarrow {}^3F_4$.[27] The relaxation of $^1D_2$ to $^3F_4$ leads to a violet emission.

The upconversion emission of the NCs were characterized in chloroform solution with fixed amount of NCs (typically 1 wt %) of variable Tm^{3+} concentration under 980 nm diode laser excitation with a total power of 38 mW.

Figure 4a shows the emission spectra of $NaY_{0.8-x}Yb_{0.2}Tm_xF_4$ nanoparticles at different doping concentrations of Tm^{3+} ions. The two strongest peaks occur at 452 nm (violet) and 476 nm (blue), corresponding to relaxation of $^1D_2 \rightarrow {}^3F_4$ and $^1G_4 \rightarrow {}^3H_6$, respectively. The intensity increases slightly when the Tm^{3+} concentration is increased from 0.05 to 0.2 molar fraction and then decreases with further increase of Tm^{3+} concentration. It is reasonable to assume that if the Tm^{3+} ion concentration is too low, there will not be enough Tm^{3+} ion to be populated or excited.[2,3] At this point, the emission intensity increases with increasing number of Tm^{3+} ions in the system. On the other hand, further increase the Tm^{3+} concentration beyond a certain threshold can lead to a decrease in the emission intensity. This is partly because a cross-relaxation mechanism exists between Tm^{3+} ions that can lead to a self-quenching effect: the increase of the Tm^{3+} concentration leads to a decrease in the distance between adjacent Tm^{3+} ions and an increase in the probability of cross-relaxation that reduces radiative relaxation, and thus suppresses the upconversion emission in high Tm^{3+} ion concentrated samples. At the same time, for a given overall excitation energy, the excitation received by individual Tm ions decreases with increasing Tm doping concentrations, which could also contribute to the weakened Tm emission.[28–30] Plotting the upconversion emission intensity normalized by the number of Tm^{3+} ions as a function of Tm^{3+} concentration, a monotonic decrease in intensity could be observed (Fig. 4c), suggesting that the cross-relaxation between neighboring Tm^{3+} ions exists in all samples include the very low-dope samples.

Figure 4a also shows that the preferred emission wavelength also changes from blue to violet with increasing the Tm^{3+} concentration. The digital camera images of NCs fluorescence clearly show different colors (from blue to violet) for the samples with increasing Tm^{3+} ion doping concentration (Fig. 4b). Plotting the ratio of violet vs. blue emission ($f_{v/b}$) shows a monotonic increase with the increasing Tm^{3+} ion concentration (Fig.

4d). This colour change as a function of Tm^{3+} ion concentration may be attributed to possible cross-relaxation processes: $^1G_4 \rightarrow {}^3F_4$ and $^3H_4 \rightarrow {}^1D_2$; and $^1G_4 \rightarrow {}^1D_2$ and $^3H_4 \rightarrow {}^3F_4$. These cross relaxation processes decrease $^1G_4$ population and increase $^1D_2$ population. Therefore, with increasing Tm^{3+} ion concentration and increasing probability of cross-relaxation, one would expect to see relatively stronger violet emission originated from $^1D_2$ state and weaker blue emission originated from $^1G_4$ state, resulting in an increase in violet/blue ratio ($f_{v/b}$) with the increase of Tm^{3+} concentration.

Additionally, we have further explored a simpler $NaYbF_4$:Tm system, using $NaYbF_4$ as the matrix and Tm as the dopant, and investigated the emission intensity vs. doping concentration. Figure 5a shows the emission spectra of a series of $NaYbF_4$:Tm NCs with variable Tm^{3+} concentration. Interestingly, only one dominant emission peak at 452 nm can be seen in this system. A maximum violet over blue emission ratio of 5.5 is observed. Removing Y^{3+} ion away from the system increases the Yb^{3+} ionconcentration, which makes it possible that cross-relaxation between Tm^{3+} ions to Yb^{3+} ions can also take place, reducing the population in $^1G_4$ state in a more significant way than $^1D_2$ state,[31] and thus significantly suppress 476 nm emission from $^1G_4$ state, leaving the 452 nm (violet) emission from the $^1D_2$ state the only dominant peak here.

The spectra in Fig. 5a also show that the best intensity is observed in sample with composition of $NaYb_{0.99}Tm_{0.01}F_4$; an additional decrease or increase in the Tm^{3+} concentration will result in a decrease in overall upconversion intensity. Normalizing the emission intensity by the number of Tm^{3+} ions, a monotonic decrease of the emission intensity vs. doping concentration could be easily observed (Fig. 5b), which is consistent with the result shown in Fig. 4c, suggesting the cross-relaxation between adjacent Tm^{3+} ions is primarily responsible for the self-quenching and the decrease of emission intensity at high Tm^{3+} concentration.

Lastly, we have also used confocal microscope to investigate the upconversion emission from individual NCs. To this end, the NCs were first spin-coated onto a glass slide. The reflection image of the NCs on glass slide shows well separated NCs or NC clusters (Fig. 6a). SEM image of a similar sample prepared on silicon wafer further shows the NCs are either single NCs or a few NC clusters (inset, Fig. 6a). Importantly, confocal photoluminescence image (Fig. 6b) clearly shows strong emission from the NCs when excited with 980 nm laser, with each bright spot in the image corresponding to emission from one or a few NCs. These studies clearly show that upconversion emission from individual NCs can be readily visualized by a confocal microscope, which is of significance for exploring them as fluorescence tags for biomedical imaging.

In summary, we successfully prepared $NaYF_4$:Yb/Tm hexagonal plate NCs with controlled composition by varying the doping concentration when synthesizing the NCs. Photoluminescence studies show strong upconversion emission in blue and violet region from the NCs when excited with 980 nm light. Importantly, the overall emission intensity and relative ratio of these two emission colours can be readily tuned by varying the exact RE^{3+} doping concentration. These studies demonstrate a rational approach to tune the upconversion emission from rare earth element doped nanomaterials, and can impact broadly from energy harvesting, energy conversion to biomedical imaging and therapeutics.

Acknowledgments

X.D. acknowledges support by the NIH Director's New Innovator Award Program, part of the NIH Roadmap for Medical Research, through grant number 1DP2OD004342-01. We acknowledge Electron Imaging Center for Nanomachines (EICN) at UCLA for the support of TEM. Confocal laser scanning microscopy was performed at the CNSI Advanced Light Microscopy/Spectroscopy Shared Resource Facility at UCLA, supported with funding from

NIH-NCRR shared resources grant (CJX1-443835-WS-29646) and NSF Major Research Instrumentation grant (CHE-0722519). We acknowledge Dr. Matthew Schibler for technical support on the confocal miscroscope.

References

1. Blasse, G.; Grabmaier, BC. Luminescent Materials. Berlin: Springer; 1994.
2. Auzel F. Chem. Rev. 2004; 104:139. [PubMed: 14719973]
3. Wang F, Liu X. Chem. Soc. Rev. 2009; 38:976. [PubMed: 19421576]
4. Lim SF, Riehn R, Ryu WS, Khanarian N, Tung CK, Tank D, Austin RH. Nano Lett. 2006; 6:169. [PubMed: 16464029]
5. Chatterjee DK, Rufaihah AJ, Zhang Y. Biomat. 2008; 29:937.
6. Chatterjee DK, Fong LS, Zhang Y. Advanced Drug Delivery Reviews. 2008; 60:1627–1637. [PubMed: 18930086]
7. Wang LY, Yan RX, Huo ZY, Wang L, Zeng JH, Bao J, Wang X, Peng Q, Li YD. Angew. Chem. Int. Ed. 2005; 44:6054.
8. Wang F, Tan WB, Zhang Y, Fan XP, Wang MQ. Nanotech. 2006; 17:R1.
9. Mirkin CA, Letsinger RL, Mucic RC, Storhoff JJ. Nature. 1996; 382:607. [PubMed: 8757129]
10. Seifert JL, Connor RE, Kushon SA, Wang M, Armitage A. J. Am. Chem. Soc. 1999; 121:2987.
11. Chan WCW, Nie SM. Science. 1998; 281:2016. [PubMed: 9748158]
12. Mai HX, Zhang YW, Si R, Yan ZG, Sun LD, You LP, Yan CH. J. Am. Chem. Soc. 2006; 128:6426. [PubMed: 16683808]
13. Ehlert O, Thomann R, Darbandi M, Nann T. ACS Nano. 2008; 2:120. [PubMed: 19206555]
14. Gamelin DR, Gudel HU. Top. Curr. Chem. 2001; 214:1.
15. Mai HX, Zhang YW, Sun LD, Yan CH. J. Phys. Chem. C. 2007; 111:13730.
16. Mai HX, Zhang YW, Sun LD, Yan CH. J. Phys. Chem. C. 2007; 111:13721.
17. Nagel G, Szellas T, Huhn W, Kateriya S, Adeishvili N, Berthold P, Ollig D, Hegemann P, Bamberg E. Proc. Natl. Acct. Sci. 2003; 100:13940.
18. Wang LY, Li YD. Chem. Master. 2007; 19:727.
19. Liang LF, Wu H, Hu HL, Wu MM, Su Q. J. Alloys Compd. 2004; 368:94.
20. Aebischer A, Hostettler M, Hause J, Kramer K, Weber T, Gudel HU, Buergi HB. Angew. Chem. Int. Ed. 2006; 45:2802.
21. Kramer KW, Biner D, Frei G, Gudel HU, Hehlen MP, Luthi SR. Chem. Mater. 2004; 16:1244.
22. Heer S, Kompe K, Gudel HU, Haase M. Adv. Mater. 2004; 16:2102.
23. Boyer JC, Vetrone F, Cuccia LA, Capobianco JA. J. Am. Chem. Soc. 2006; 128:7444. [PubMed: 16756290]
24. Li ZQ, Zhang Y. Angew. Chem. Int. Ed. 2006; 45:7732.
25. Zhang H, Li Y, Ivanov IA, Qu Y, Huang Y, Duan X. Angew Chemie Intl. Ed. 2010; 16:2865.
26. Chem. Commun. 2010
27. Wang G, Qin W, Wang L, Wei G, Zhu P, Kim R. Optics Exp. 2008; 16:11907.
28. Wang F, Liu XG. J. Am. Chem. Soc. 2008; 130:5642. [PubMed: 18393419]
29. Wang F, Han Y, Lim CS, Lu Y, Wang J, Xu J, Chen H, Zhang C, Hong M, Liu X. Nature. 2010; 463:1061. [PubMed: 20182508]
30. Yin A, Zhang Y, Sun L, Yan C. Nanoscale. 2010; 2:953. [PubMed: 20644777]
31. Ryba-Romanowski W, Golab S, Dominiak-Dzik G, Zelechower M, Gabrys-Pisarska J. J. Alloys Compd. 2001; 325:215.

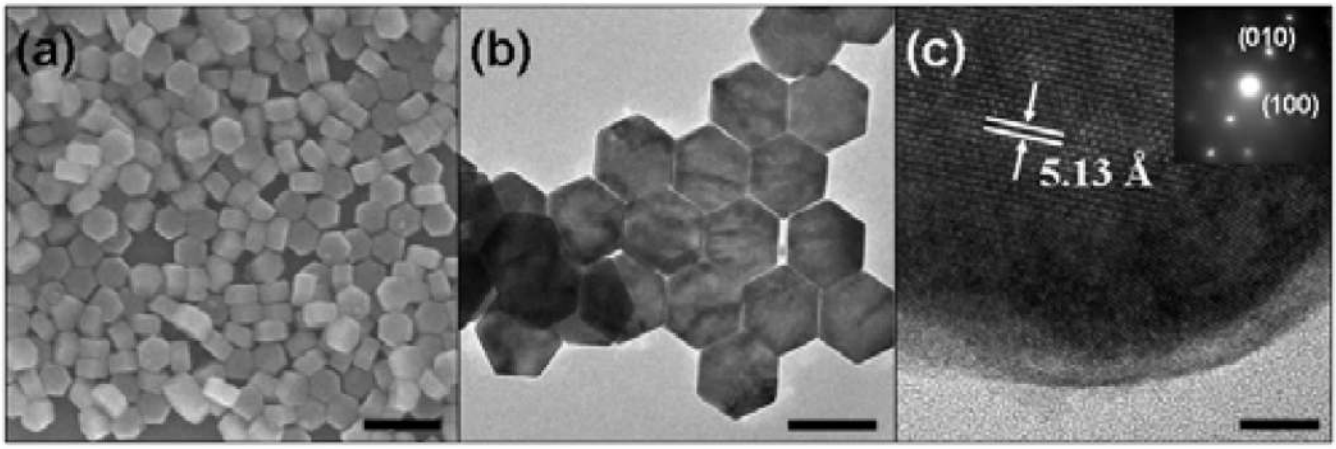

Fig. 1.
(a) SEM, (b)TEM, (c and inset) HRTEM and SAED images of $NaYbF_4$:Tm NPs with uniform hexagonal shape (the scale bars correspond to 400 nm, 200 nm and 5 nm, respectively).

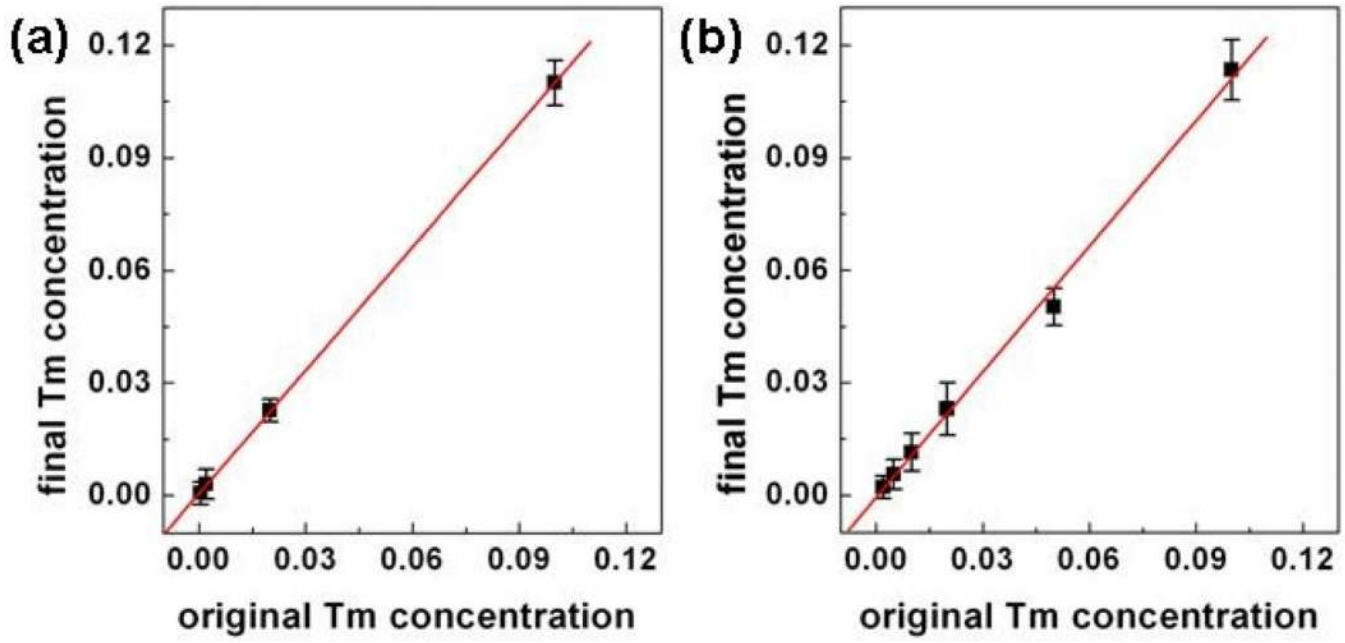

Fig. 2.

Diagram of final Tm^{3+} concentration versus original Tm^{3+} concentration in (a) $NaY_{0.8-x}Yb_{0.2}Tm_xF_4$ NCs and (b) $NaYb_{1-x}Tm_xF_4$ NCs.

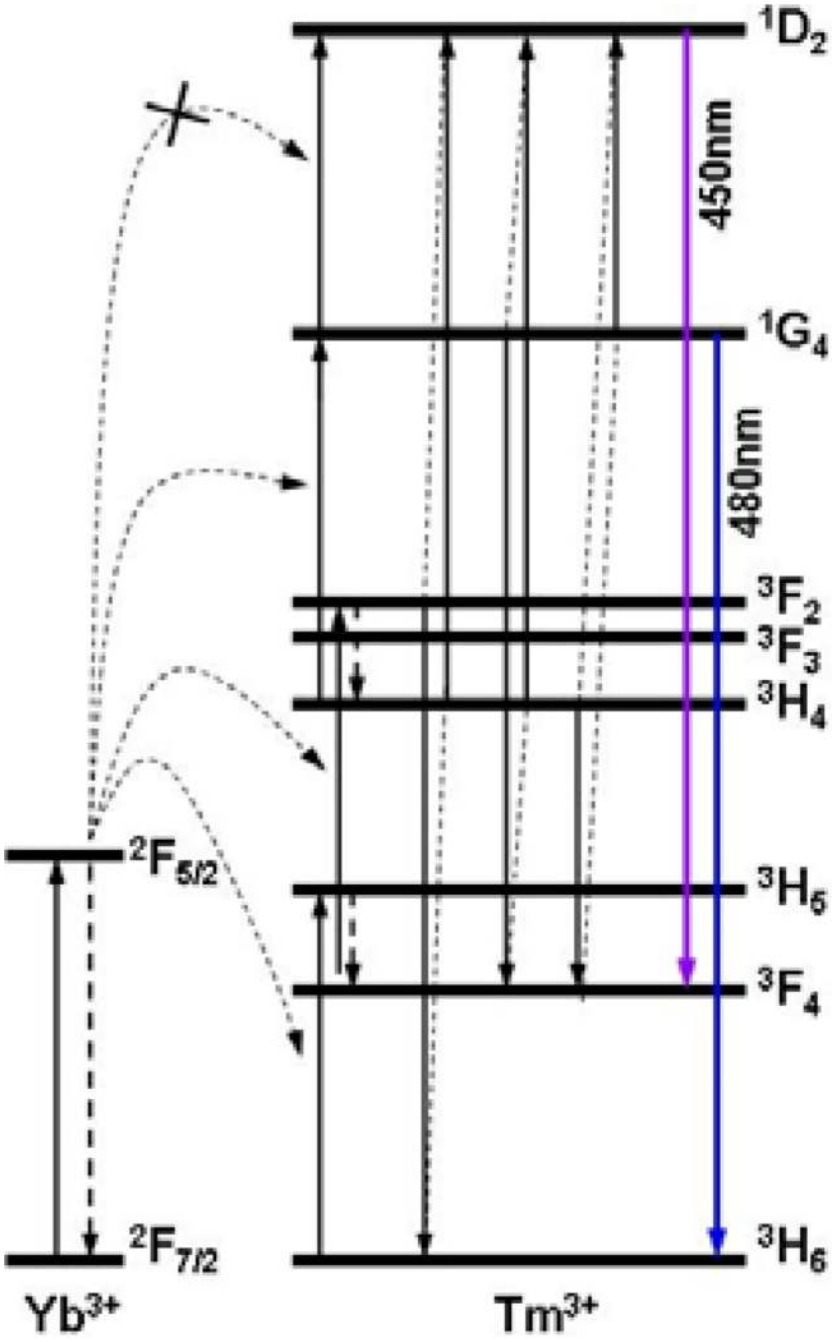

Fig. 3.

Schematic illustration of the energy levels invovled in the upconversion process of Tm^{3+} with Yb^{3+} as the promoter for NaYF4:Yb,Tm NCs.

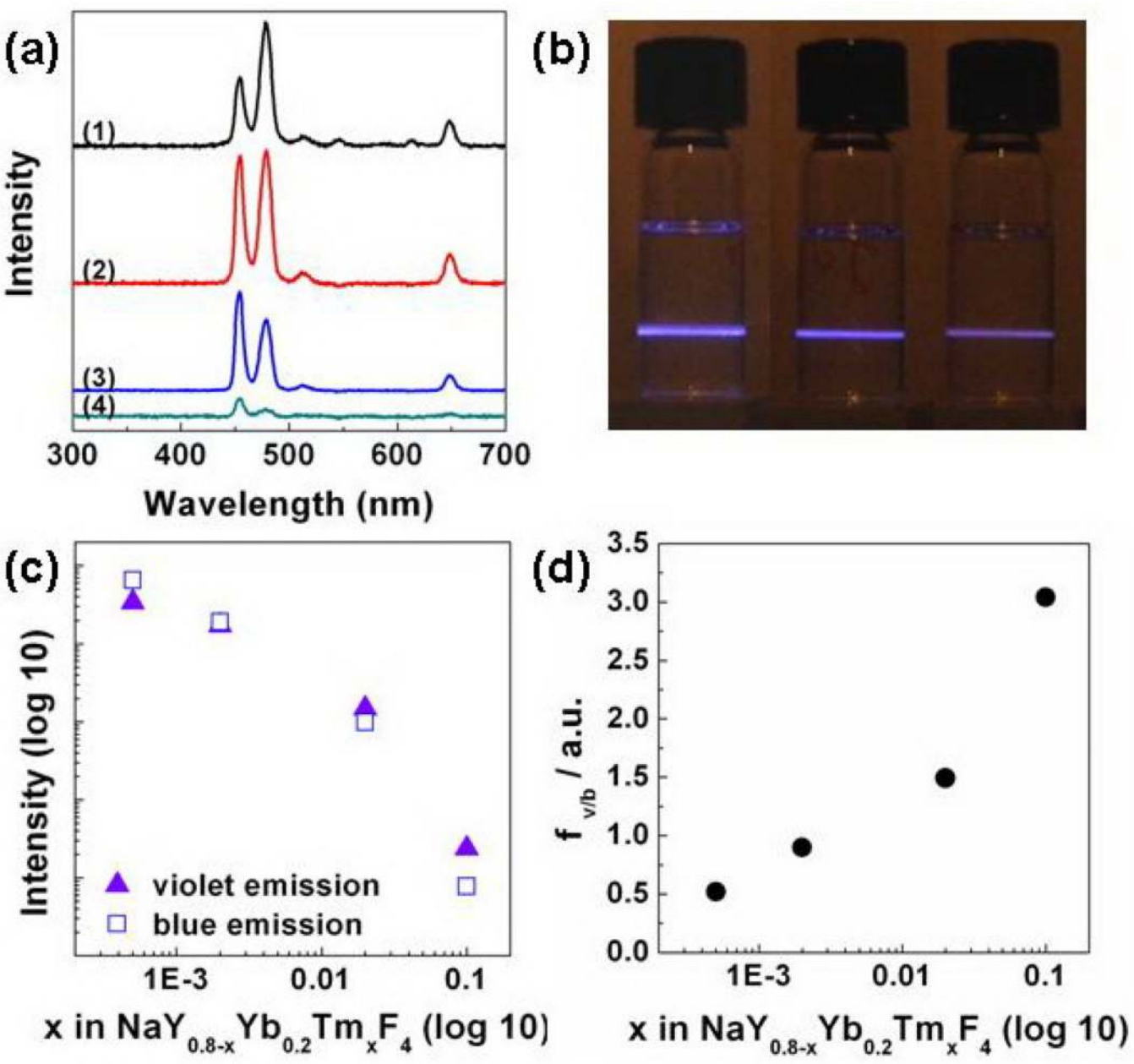

Fig. 4.

(a) Upconversion emission spectra of $NaY_{0.8-x}Yb_{0.2}Tm_xF_4$ NCs with different Tm^{3+} concentrations, x = 0.0005, 0.002, 0.02, 0.1, for (1), (2), (3), (4) respectively. (b) Digital camera pictures of $NaY_{0.7995}Yb_{0.2}Tm_{0.0005}F_4$, $NaY_{0.798}Yb_{0.2}Tm_{0.002}F_4$ and $NaY_{0.78}Yb_{0.2}Tm_{0.02}F_4$ (from left to right) samples under 980 nm excitation. (c) Upconversion emission intensity (normalized by Tm^{3+} ion concentration) versus doping concentration of Tm^{3+} in $NaY_{0.8-x}Yb_{0.2}Tm_xF_4$ NCs. (d) Diagram of violet to blue emission ($f_{v/b}$) ratio versus Tm^{3+} doping concentration in $NaY_{0.8-x}Yb_{0.2}Tm_xF_4$ NCs.

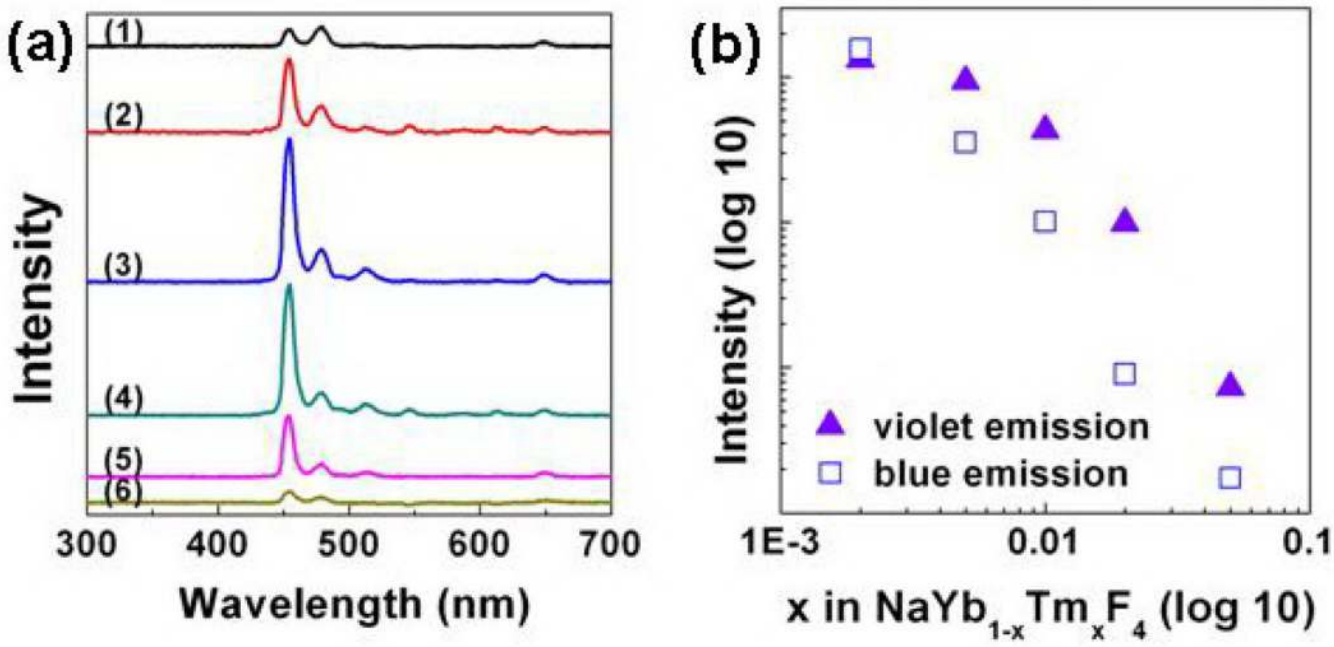

Fig. 5.

(a) Upconversion emission spectra of $NaYb_{1-x}Tm_xF_4$ NCs with different Tm^{3+} concentrations, x = 0.002, 0.005, 0.01, 0.02, 0.05, 0.1, for (1), (2), (3), (4), (5), (6) respectively. (b) Tm^{3+} normalized upconversion emission intensity versus doping concentration of Tm^{3+} in $NaYb_{1-x}Tm_xF_4$.

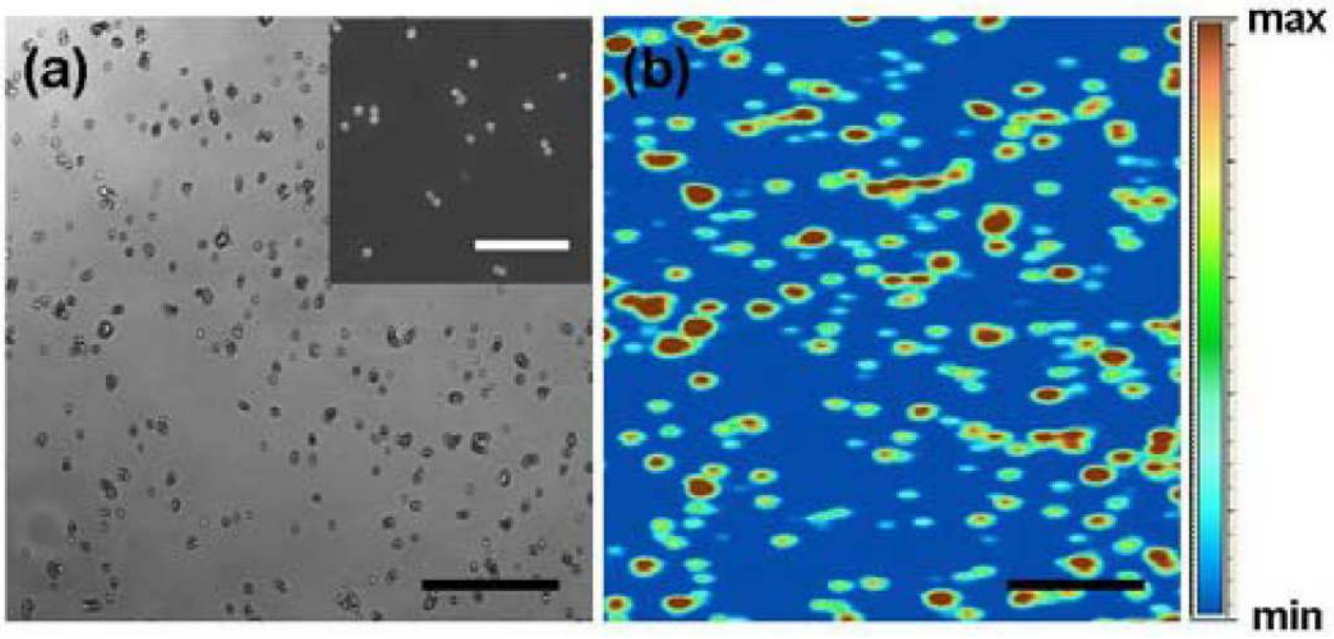

Fig. 6.

(a) Reflection image of NCs on glass substrate. (inset) SEM image of a similar sample prepared on silicon wafer. (b) Confocal photoluminescence image of the upconversion nanocrystals shown in (a). (Scale Bar: 25 μm for (a) and (b), and 5μm for the inset).